NJC

Accepted Manuscript

This article can be cited before page numbers have been issued, to do this please use: R. Hashemi Fath and S. J. Hoseini, *New J. Chem.*, 2017, DOI: 10.1039/C6NJ02771G.

ROYAL SOCIETY OF CHEMISTRY

rsc.li/njc

View Article Online
DOI: 10.1039/C6NJ02771G

Synthesis of thiospinel $CuCo_2S_4$ and $CuCo_2S_4$/ reduced-graphene oxide nanohybrids as highly effective catalysts for the Sonogashira reaction†

Roghayeh Hashemi Fath and S. Jafar Hoseini*

Department of Chemistry, Faculty of Sciences, Yasouj University, Yasouj 7591874831, Iran

Abstract

Formation of carbon – carbon bond using transition metal catalyzed Sonogashira coupling reaction is an indispensable tool in synthetic organic chemistry. Initially complexes of Pd were used as catalysts, however advances in catalyst design fuelled the development of Cu catalysts, which are cheaper and more environmentally benign than the complexes of Pd. This is the first paper that reports the application of thiospinels in the Sonogashira reaction. Thiospinel $CuCo_2S_4$ and $CuCo_2S_4$/ reduced-graphene oxide (RGO) nanohybrids were firstly synthesized through a simple solvothermal approach. Our studies show that all of these nanohybrids are suitable for the Sonogashira reaction in water at room temperature. Compared to classical reactions, this method consistently has the advantages of a green solvent, short reaction times, low catalyst loading, high yields and reusability of the catalysts and a facile method for the preparation of the catalysts. The $CuCo_2S_4$ and $CuCo_2S_4$/RGO nanohybrids showed highly improved catalytic activity toward aryl chloride derivatives as compared with other catalysts that have been reported.

---

* Corresponding author: E-mail: jhosseini@yu.ac.ir, sjhoseini54@yahoo.com, Fax: +98 74 33342172; Tel: +98 74 33223048.

View Article Online
DOI: 10.1039/C6NJ02771G

Introduction

The Sonogashira reaction is used in numerous syntheses of natural products, for instance, enediyne antibiotics, as well as in the preparation of conducting polymers, liquid crystals and other engineering materials.[1,2] An important trend in modern development of synthetic ways is the search for cheaper starting materials, ligands, and catalysts. For example copper derivatives are replacing very expensive palladium in the cross-coupling reaction and related processes.[3] The Pd-free Cu-catalyzed Sonogashira cross-coupling reaction has been attracting a significant interest for last two decades since its discovery.[4] Large number of new catalytic systems based on copper have been proposed. These catalysts involve not only phosphines,[5] but also O- and N-donating ligands,[6] some of which are quite simple and readily available. Following principles of green chemistry, aqueous,[7] solvent-free[8] and ligand-free[9] systems were reported. In this study, to the best of our knowledge, there is no report concerning the application of thiospinels in the Sonogashira reaction.

Sulfides of transition metal that adopt the spinel crystal structure are generally referred to as thiospinels. Thiospinels have an ideal formula of MM'_2S_4, where M and M′ are normally divalent and trivalent metal cations, respectively, though other oxidation numbers and off-stoichiometry formulas sometimes can be accommodated.[10] Among the most common thiospinels are single metal systems (M = M′), such as Co_3S_4, Ni_3S_4, and Fe_3S_4. Exchange of some of the cobalt metal in Co_3S_4 with copper metal generates a solid solution, ultimately forming the end member $CuCo_2S_4$. $CuCo_2S_4$, which is the mineral carrollite, is a normal spinel, with Cu occupying the tetrahedral sites and Co occupying octahedral site. Thiospinels are widely studied for their electronic, magnetic, and catalytic properties.[11]

View Article Online
DOI: 10.1039/C6NJ02771G

Graphene, a single atom thick layer of sp^2 hybridized carbon atoms tightly packed into a two-dimensional honeycomb lattice, is the basic building unit for graphitic materials of all other dimensionalities.[12] The properties of graphene such as chemical, high thermal, and mechanical stability as well as high surface area represent desirable characteristics as 2D support layers for metallic nanoparticles (NPs) in heterogeneous catalysis, chemical sensors, fuel cells, and hydrogen storage applications.[13] Recently, graphene, graphene oxide (GO) and functionalized GO have been considered as excellent carbon supports for metal-catalyzed carbon–carbon coupling applications.[14]

In this study, we have prepared thiospinel $CuCo_2S_4$ and $CuCo_2S_4$/ reduced-graphene oxide (RGO) nanohybrids *via* a facile solvothermal method. Reducing the consumption of precious metals such as Pd by bimetallization with a low-cost and non-noble metal is a popular approach. In this article, using Cu and Co metals can decrease the cost of catalysts. Then, these nanohybrids are used as non-phosphine catalysts for the Sonogashira reaction in water. The $CuCo_2S_4$/RGO nanohybrid was used as efficient catalyst in the Sonogashira coupling reaction, with the lowest loading of 0.4 mol% of Cu, the reaction was completed after 20 min at room temperature (r.t.). These results demonstrate the remarkable catalytic activity of $CuCo_2S_4$/RGO nanohybrid with a turnover number (TON) of 240 and turnover frequency (TOF) of 720 h^{-1}. Metal–metal interaction has a significant effect on oxidative addition and reductive elimination as key steps in Sonogashira reaction. Elements of the first-row of transition metals facilitate the reductive elimination step as final step in Sonogashira reaction. Thiospinel $CuCo_2S_4$ and $CuCo_2S_4$/RGO nanohybrids showed higher catalytic activity in the Sonogashira reaction due to the appropriate interaction between copper and cobalt metals.

View Article Online
DOI: 10.1039/C6NJ02771G

Experimental

All of the chemical compounds were purchased from Sigma-Aldrich and Merck companies. The powder X-ray diffraction (XRD) patterns were obtained by a Bruker AXS (D8, Advance) instrument employing the reflection Bragg–Brentano geometry with Cu-Kα radiation. The surface atomic concentration and chemical composition of the samples were investigated by X-ray photoelectron spectroscopy (XPS) equipped with an Al Kαx-ray source at energy of 1486.6 eV in an ultrahigh vacuum (UHV) system with a base pressure lower than 2×10^{-9} Torr. Transmission electron microscopy (TEM) images were taken with a Philips CM-10 microscope operated at 100 kV. The loading amount of copper was determined using an inductively coupled plasma (ICP) analyzer (Varian, Vista-Pro). ^{1}H NMR spectra were taken with a Bruker 400 MHz ultra-shield spectrometer using $CDCl_3$ as the solvent. ^{13}C NMR was recorded on a Varian 100 MHz spectrometer.

Preparation of $CuCo_2S_4$/RGO nanohybrid

The GO was synthesized from natural graphite flakes by a modified Hummers method.[14a-c, 15] In a typical synthesis of $CuCo_2S_4$/RGO nanohybrid, $Co(NO_3)_2$ (0.6 mmol) and $Cu(NO_3)_2$ (0.3 mmol) were dissolved in 60 ml of GO/ ethylene glycol (EG) suspension and reflux at 80 °C for 2 h. Then, thiourea (0.18 mmol) was added into the above suspension. Finally, the mixture was transferred into an autoclave (75 ml), and heated at 200 °C for 8 h. After being cooled to room temperature, the mixture was centrifuged and black crystals were separated, washed with water and ethanol and dried in vacuum at 60 °C for 8 h. For comparisons, $CuCo_2S_4$ nanoparticle was synthesized using a reported procedure.[16]

View Article Online
DOI: 10.1039/C6NJ02771G

General procedure for Sonogashira carbon–carbon coupling reaction

Aryl halide (0.5 mmol) and phenylacetylene (0.75 mmol) were added to a flask containing the catalyst (3 mg) and K_2CO_3 (1 mmol) in 5 ml of H_2O at room temperature. After the reaction was completed (monitored by TLC), the catalyst was separated and dichloromethane (3 × 5 ml) was added to the reaction solution. The organic layer was separated and dried over anhydrous $MgSO_4$. Evaporation of the solvent gave the desired organic product, then analyzed by ^{1}H NMR spectra with those of authentic sample and the details are given in the ESI.† The turnover number (TON = mol of product per mol of catalyst) and turnover frequency (TOF = TON per time (h)) were calculated on the basis of the amount of diarylacetylene product formed.

Results and discussion

Physicochemical characterization of the catalysts

$CuCo_2S_4$/RGO nanohybrid was prepared by a simple solvothermal route using $Co(NO_3)_2$, $Co(NO_3)_2$, thiourea, and GO as precursors in EG. The polyol (such as EG) method is usually employed to synthesize nanosized materials.[17] It is known that a catalyst with amorphous or nanocrystalline phase would be rendered a great performance on account of abundant accessible active sites.[18] In this the reaction, EG acts as a medium reductant to get RGO and also the solvent with a chelating effect, which avoids agglomeration of NPs; GO provides large amounts of defects/functional groups as nucleation sites for in situ growth of $CuCo_2S_4$ nanohybrids. Thiourea is intended for the formation of sulfides of metal. The solvothermal procedure is of significant importance, affording the crystallization of $CuCo_2S_4$ nanohybrid, the reduction of GO, and the final formation of $CuCo_2S_4$/RGO nanohybrid.

View Article Online
DOI: 10.1039/C6NJ02771G

The crystallographic structures of $CuCo_2S_4$ and $CuCo_2S_4$/RGO nanohybrids synthesized in EG solvent were analysed by XRD (Fig. 1). All diffraction peaks reveal the successful formation of the carrollite structure phase of $CuCo_2S_4$. The main diffraction peaks of (022), (113), (004), (224), (115), and (044) are attributable to carrollite phase of the $CuCo_2S_4$ structure (Fig 1a).[16,19] Fig. 1b shows the XRD pattern recorded for $CuCo_2S_4$/RGO nanohybrid. The first peak located at 2Θ in 25 is attributable to RGO, and other diffraction peaks confirm the carrollite phase for the $CuCo_2S_4$.

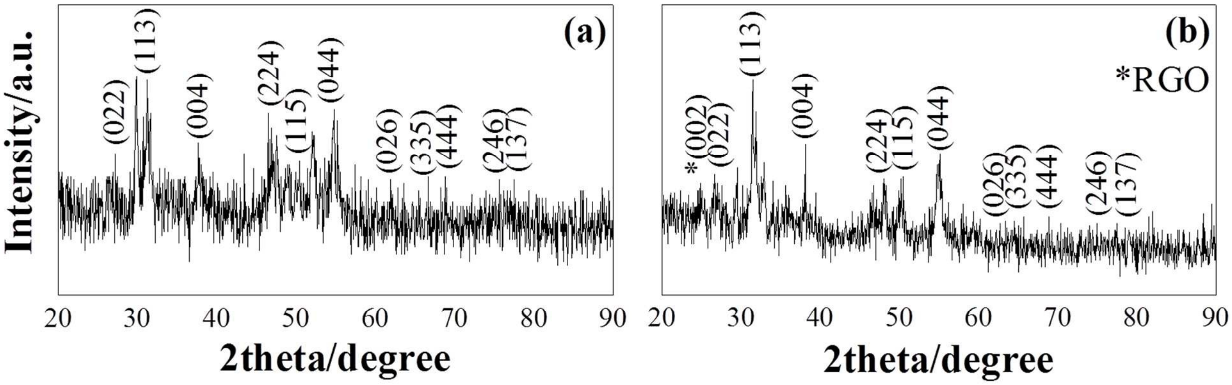

Fig. 1 XRD patterns of (a) $CuCo_2S_4$, and (b) $CuCo_2S_4$/RGO nanohybrids.

XPS was used to determine the composition of the as-prepared $CuCo_2S_4$/RGO nanohybrid. Fig. 2 shows the XPS spectra of Cu 2p and Co 2p. The spin-orbit doublet corresponding to Cu $2p_{1/2}$ and Cu $2p_{3/2}$ is readily observed in the Cu 2p region at 952.1 and 932.0 eV with a spin–orbit splitting value of 20.1 eV, respectively, and the Cu $2p_{3/2}$ curve region was assigned to Cu^+, Cu^{2+} and Cu^{3+} (Fig. 2a).[16] As shown in Fig. 2b, two prominent peaks at binding energies of 779.7 and 795.3 eV corresponded to the Co $2p_{3/2}$ and Co $2p_{1/2}$ spin–orbit peaks with a spin–orbit splitting value of 15.6 eV, respectively, which confirmed the existence of two kinds of cobalt oxidation state: Co^{2+} and Co^{3+}.[16]

View Article Online
DOI: 10.1039/C6NJ02771G

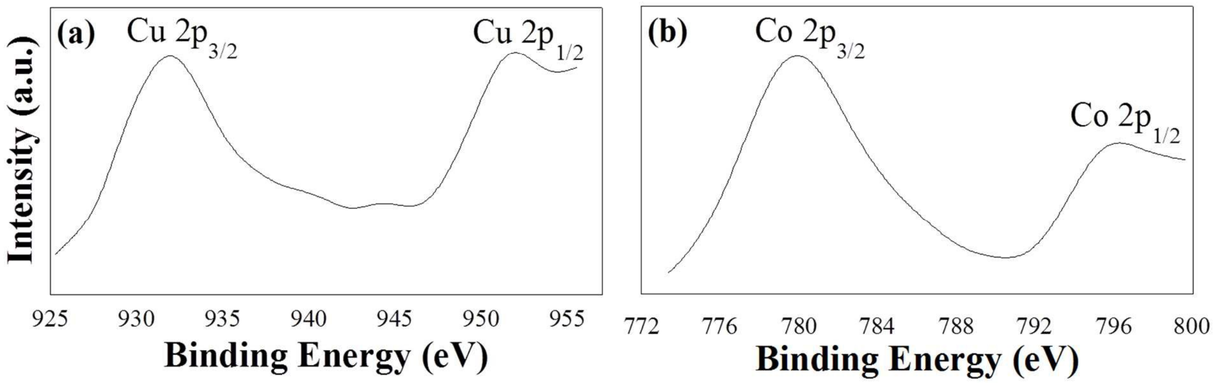

Fig. 2 XPS curves of $CuCo_2S_4$/RGO nanohybrid (a) Cu 2p and (b) Co 2p.

Fig. 3 shows TEM images of the as-prepared $CuCo_2S_4$/RGO nanohybrid, that metal sulfide NPs are uniformly decorated on graphene sheets without detachment and aggregation.

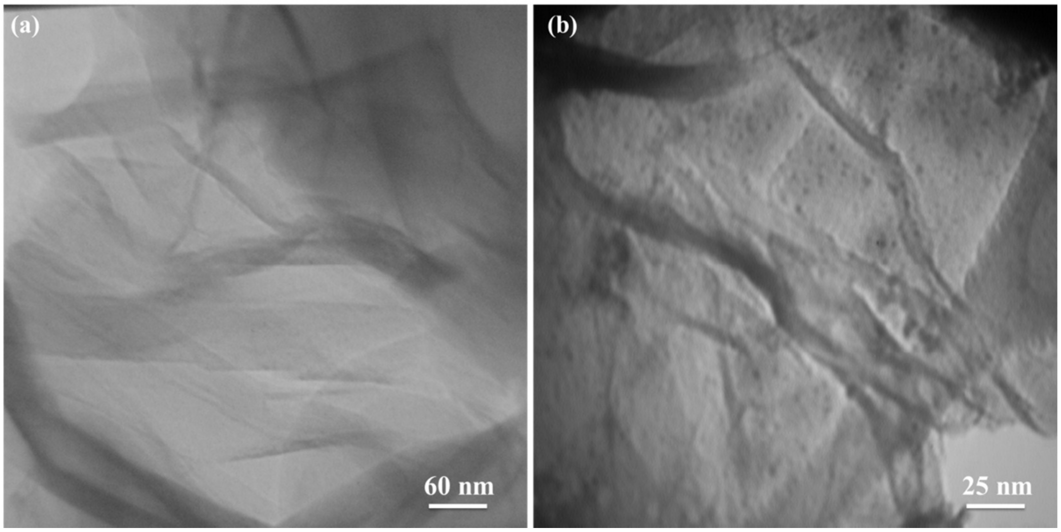

Fig. 3 (a and b) TEM images of $CuCo_2S_4$/RGO nanohybrid.

Catalytic activity

The formation of carbon–carbon bond is one of the most fundamental reactions for the construction of molecular frameworks in organic chemistry. Therefore, in the present project, we

View Article Online
DOI: 10.1039/C6NJ02771G

studied the role of the prepared catalysts toward the Sonogashira coupling reaction in the presence of the H_2O solvent. The heterogeneous catalysts are used in the present project. K_2CO_3 was used as a base for optimizing the reaction conditions. When the reaction was tested at room temperature, the polar solvent H_2O gave an excellent yield. Therefore, in this study, we have investigated the role of the prepared catalysts toward the Sonogashira reaction in the presence of the H_2O solvent at room temperature (Table 1).

Table 1 Sonogashira cross-coupling of aryl halides with phenylacetylene catalyzed by the $CuCo_2S_4$ and $CuCo_2S_4$/RGO nanohybrids

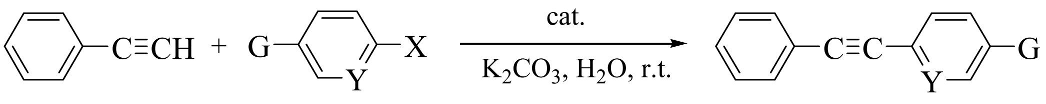

Y = C, N
G = H, Me, NO_2
X = Cl, Br, I

1a; Y = C, G = H
1b; Y = C, G = Me
1c; Y = C, G = NO_2
1d; Y = N, G= H

Entry	Substrate	Product	Cat.	Time (min)	Yields (%)[a]	TON[b]	TOF[b](h^{-1})
1	C_6H_5I	1a	$CuCo_2S_4$[c]	35	93	46.5	79.7
			$CuCo_2S_4$/RGO[d]	20	96	240	720
2	C_6H_5Br	1a	$CuCo_2S_4$	55	85	42.5	46.4
			$CuCo_2S_4$/RGO	33	90	225	409.1
3	4-MeC_6H_4Br	1b	$CuCo_2S_4$	190	67	33.5	10.6
			$CuCo_2S_4$/RGO	125	75	187.5	90
4	C_6H_5Cl	1a	$CuCo_2S_4$	155	65	32.5	12.6
			$CuCo_2S_4$/RGO	50	65	162.5	195
5	4-$NO_2C_6H_4Cl$	1c	$CuCo_2S_4$	115	70	35	18.3
			$CuCo_2S_4$/RGO	45	80	200	266.7
6	C_5H_4NCl	1d	$CuCo_2S_4$	580	70	35	3.6
			$CuCo_2S_4$/RGO	320	80	200	37.5

[a] Isolated yields. [b] See Experimental section for the calculation of TONs and TOFs. [c] $CuCo_2S_4$ (2 mol% of Cu). [d] $CuCo_2S_4$/RGO (0.4 mol% of Cu).

View Article Online
DOI: 10.1039/C6NJ02771G

The Sonogashira reaction of activated aryl iodide and bromide with different substituents also gave good yields with yields ranging from 67 to 96%, as shown in Table 1, entries 1-3. In addition, the yields for chlorobenzene, 1-chloro-4-nitrobenzene and 3-chloropyridine were low with yields ranging from 65 to 80%, as shown in Table 1, entries 4-6. The results showed that the aryl iodide and bromide are more suitable substrates for diarylacetylene synthesis.

Also, we use some other ways to improve the yield of reaction of chlorobenzene with phenylacetylene. For this purpose, the coupling reaction of chlorobenzene with phenylacetylene in the presence of $CuCo_2S_4$/RGO nanohybrid catalyst was tested at various solvents and temperatures. The results are shown in Table 2. The reaction went in the presence of $CuCo_2S_4$/RGO nanohybrid catalyst in H_2O at high temperature (80 °C) and the desired product was obtained in 73% yield (Table 2, entry 2). The solvents such as EtOH, H_2O:EtOH (1:1), THF, H_2O:THF (2:1) and toluene also afforded low yields of the coupling product.

Table 2 Solvent and temperature effects on the Sonogashira reaction of chlorobenzene with phenylacetylene catalyzed by the $CuCo_2S_4$/RGO nanohybrid[a]

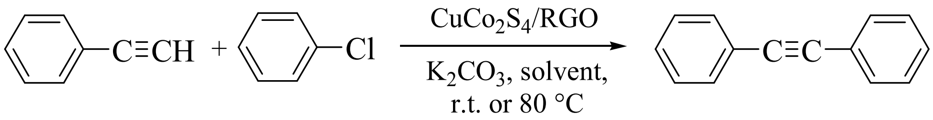

Entry	Solvent	Yield (%)[b]	
		r.t. °C	80 °C
1	EtOH	30	43
2	H_2O	65	73
3	H_2O:EtOH (1:1)	42	59
4	THF	trace	15
5	H_2O:THF (2:1)	36	52
6	Toluene	trace	trace

[a] Reaction conditions: 0.50 mmol of chlorobenzene, 0.75 mmol of phenylacetylene, 1.00 mmol of K_2CO_3, 5.0 ml of solvent, reaction time 50 min. [b] Isolated yield.

View Article Online
DOI: 10.1039/C6NJ02771G

Also, the Sonogashira reaction of bromobenzene with phenylacetylene in water at room temperature was examined by $Cu(NO_3)_2$, $Cu(NO_3)_2$ + $Co(NO_3)_2$ and $Cu(NO_3)_2$ + $Co(NO_3)_2$ + thiourea as catalyst. The results are shown in Table 3.

Table 3 Sonogashira cross-coupling of bromobenzene with phenylacetylene catalyzed by the $Cu(NO_3)_2$, $Cu(NO_3)_2$ + $Co(NO_3)_2$ and $Cu(NO_3)_2$ + $Co(NO_3)_2$ + thiourea[a]

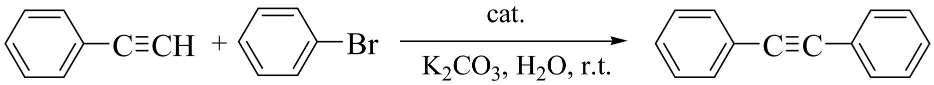

Entry	Cat.	Yield (%)[b]
1	$Cu(NO_3)_2$	31
2	$Cu(NO_3)_2$ + $Co(NO_3)_2$	37
3	$Cu(NO_3)_2$ + $Co(NO_3)_2$ + thiourea	39

[a] 0.5 mmol of bromobenzene, 0.75 mmol of phenylacetylene, 1.00 mmol of K_2CO_3, 5 ml of H_2O, reaction time 55 min. [b] Isolated yield.

The $CuCo_2S_4$ and $CuCo_2S_4$/RGO nanohybrids are used as heterogeneous catalysts in the present project. The results showed that $Cu(NO_3)_2$, $Co(NO_3)_2$ and thiourea act as homogeneous catalysts, which has disadvantages of difficult product separation from reaction mixture, recovery of catalyst and problems associated with the recycling of the catalyst. The reaction proceeds with yields of 31%-39% in the presence of $Cu(NO_3)_2$, $Cu(NO_3)_2$ + $Co(NO_3)_2$ and $Cu(NO_3)_2$ + $Co(NO_3)_2$ + thiourea catalysts (Table 3, entries 1-3) and with yield of 85% in the presence of $CuCo_2S_4$ catalyst (Table 1, entry 2). The results showed that thiospinel $CuCo_2S_4$ nanohybrid is the better catalyst. Several recent studies have shown that the catalytic activity of metals can be improved by incorporating a second metal due to the synergistic effect. Synergistic effects were observed for the Co-Cu catalyst.[20] Transition metal based composite materials exhibit synergistic enhancements in properties like chemical activity, stability and resistance to

View Article Online
DOI: 10.1039/C6NJ02771G

poisoning for catalytic activities, which are much better than a simple combination of individual components.[21] A synergistic effect of copper and cobalt was observed over the Cu-Co-S composite nanocatalyst, which showed higher activity than either Cu salt or Cu salt and Co salt alone.

We propose that the reaction proceeds *via* proposed pathway in the scheme 1. Firstly, $CuCo_2S_4$ nanohybrid in presence of K_2CO_3 base formed Cu-acetylide intermediate. Second step of catalytic cycle is oxidative addition step and occurs between the Cu-acetylide complex and carbon-halogen (C-X) bond. The final step is the reductive elimination step where produced the our desired diarylacetylene product and $CuCo_2S_4$ catalyst.

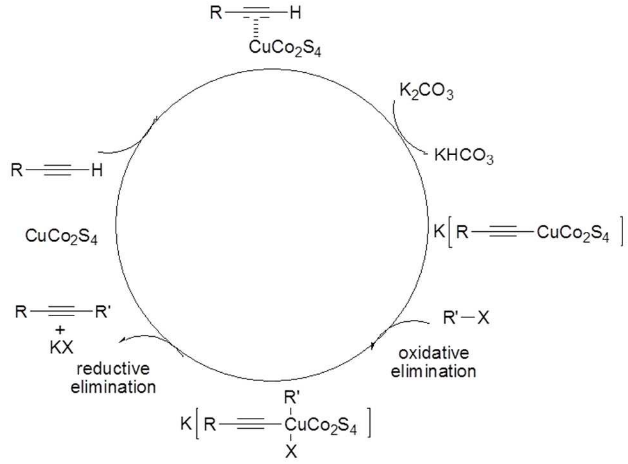

Scheme 1 Plausible mechanism of the $CuCo_2S_4$-catalyzed Sonogashira coupling.

Oxidative addition and reductive elimination are key steps in Sonogashira coupling reactions. Synergistic effects could be important in reductive elimination, migratory insertion, and nucleophilic attack on coordinated ligands,[22] so, improve the catalytic activity due to the Cu–Co interaction that accelerates the reductive elimination reaction in the last step of the reaction.

View Article Online
DOI: 10.1039/C6NJ02771G

The oxidative addition of copper into a C-X bond occurs in the order I > Br >> Cl >> F, based mainly on the strength of the C-X bond. As expected, electron-withdrawing groups on the aryl ring enhance reactivity compared to electron-donating groups. Bromobenzene is faster than 4-bromotoluene in the Sonogashira reaction because CH_3 is electron donor group and reduces oxidative addition step speed, as shown in Table 1, entries 2 and 3. Chlorobenzene is slower than 1- chloro- 4- nitrobenzene due to NO_2 group that is electron-withdrawing and cause weaken $C(sp^2)$-Cl bond and increase the speed of oxidative addition, as shown in Table 1, entries 4 and 5.

As shown in Table 1, for the reactions of aryl halides with phenylacetylene in the presence of $CuCo_2S_4$/RGO catalyst, TOF or TON factors are higher than that for the $CuCo_2S_4$ and shorter times are seen. The most activity of $CuCo_2S_4$/RGO is attributed to nanostructure of the catalyst and the precense of graphene sheets that these properties increases the surface to volume ratio of the catalyst to accelerate the reactions.

From an industrial point of view, the reusability of a catalyst is important for large-scale operation. Therefore, the reusability of the catalysts was examined in the reaction of bromobenzene with phenylacetylene in water at room temperature. Centrifugation was applied to separate the catalyst from the reaction mixture and then was washed with water and diethyl ether. $CuCo_2S_4$ and $CuCo_2S_4$/RGO nanohybrids catalysts were recovered by simple filtration from the reaction pot and can be reused successfully. The recovered catalysts were dried and checked using XRD analysis. As shown in Fig. 4, the results showed that the catalysts can be reused seven consecutive times without noticeably losing activity.

View Article Online
DOI: 10.1039/C6NJ02771G

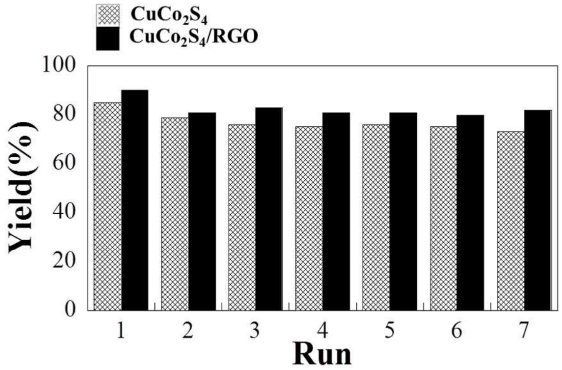

Fig. 4 Recycling result of the coupling reaction of bromobenzene with phenylacetylene in the presence of $CuCo_2S_4$ and $CuCo_2S_4$/RGO nanohybrids.

The TON and TOF is used to measure the efficiency of a catalyst. Bhaumik *et al*. reported that the Sonogashira reaction over a Pd(0)/MCoS-1 catalyst gives TOF of 78.3 h^{-1}.[23] Sardarian *et al*. reported that the Sonogashira reaction over a dendrimer-encapsulated Pd(0) supported on silica catalyst gave TOF of 67.2 h^{-1}.[24] In the current study using $CuCo_2S_4$/RGO as a catalyst, a higher TOF of 720 h^{-1} was observed for the Sonogashira reaction of iodobenzene with phenylacetylene.

We compared our results with those of the Cu metal based catalysts reported in the past few years for Sonogashira coupling reaction, taking the reactions of bromobenzene and 4-bromotoluene with phenylacetylene for Sonogashira coupling as two examples (Table 4).[25-29] Although some of them can also obtain high yields, the following factors make our catalysts superior to the others for these reactions. (i) excellent repeatability without loss of catalytic activity in the H_2O solvent at room temperature, (ii) the low-cost Cu-based catalysts were prepared by a facile and efficient method, (iii) excellent results were obtained in short reaction times using low catalyst loading.

Table 4 Catalytic performance of different Cu-based catalysts in the coupling of bromobenzene and 4-bromotoluene with phenylacetylene

Entry	G	Catalyst	Solvent	Ligand	Base	Temp (ºC)	Time (h)	Yield (%)	Ref
1	H	[ChCl][CuCl][a]	DMF	ligand-free	KOH	140	9	80	25
2	H	CuI[b]	DMF	L[c]	K_2CO_3	140-145	48	35	26
3	H	CuI[d]	DMF	DABCO[e]	Cs_2CO_3	135-140	15	91	27
4	H	CuI[f]	dioxane	ethylene diamine[g]	K_2CO_3	110	24	62	28
5	H	$Cu(OAc)_2{\cdot}H_2O$[h]	solvent-free	DAB-Ph[i]	TBAB[j]	130-135	20	57	29
6	H	$Cu(OAc)_2{\cdot}2H_2O$[k]	solvent-free	DAB-Ph[l]	TBAB[j]	140-145	26	72	29
7	H	$CuCo_2S_4$	H_2O	ligand-free	K_2CO_3	r.t.	0.92	85	This work
8	H	$CuCo_2S_4$/RGO	H_2O	ligand-free	K_2CO_3	r.t.	0.55	90	This work
9	Me	$Cu(OAc)_2{\cdot}H_2O$[h]	solvent-free	DAB-Ph[i]	TBAB[j]	130-135	19	32	29
10	Me	$Cu(OAc)_2{\cdot}2H_2O$[k]	solvent-free	DAB-Ph[l]	TBAB[j]	140-145	24	70	29
11	Me	CuI[b]	DMF	L[c]	K_2CO_3	140-145	24	51	26
12	Me	CuI[f]	dioxane	ethylene diamine[g]	KOH	110	24	60	28
13	Me	$CuCo_2S_4$	H_2O	ligand-free	K_2CO_3	r.t.	3.17	67	This work
14	Me	$CuCo_2S_4$/RGO	H_2O	ligand-free	K_2CO_3	r.t.	2.08	75	This work

[a] [ChCl][CuCl] (20 mol%), [b] CuI (20 mol %), [c] L: N,N′-dibenzyl BINAM (20 mol %), [d] CuI (10 mol %), [e] DABCO (20 mol %), [f] CuI (30 mol %), [g] 45 mol% ethylene diamine, [h] Cu(OAc) $2H_2O$ (10 mol%), [i] DAB-Ph: 1,4-Diphenyl-1,4-diazabuta-1,3-diene (20 mol%), [j] TBAB (1 equiv). 130–135 °C. [k] $Cu(OAc)_2.2H_2O$ (50 mol%), [l] DAB-Ph (100 mol%).

View Article Online
DOI: 10.1039/C6NJ02771G

Conclusions

In conclusion, a simple solvothermal method was firstly used to synthesize thiospinel $CuCo_2S_4$ and $CuCo_2S_4$/RGO nanohybrids, and exhibits a high catalytic activity in the Sonogashira coupling reaction. $CuCo_2S_4$ nanoparticles have well dispersed very small sized on GO surface, which act as the active site for the Sonogashira reactions. Furthermore, $CuCo_2S_4$ and $CuCo_2S_4$/RGO nanohybrids show a high catalytic activity toward aryl chloride derivatives. Our final goal was the synthesis of non-precious metals catalysts with both improved performance and low cost. The present method is promising for the synthesis of high performance catalysts for Sonogashira coupling reaction.

Acknowledgements

We thank the Yasouj University Research Council and the Iranian Nanotechnology Initiative Council for their support.

References

1 (*a*) L. Brandsma, S. F. Vasilevsky and H. D. Verkruijsse, Application of Transition Metal Catalysts in Organic Synthesis; Springer: Berlin, 1988; Chapter 10, pp. 179; (*b*) K. C. Nicolau and E. J. Sorensen, Classics in Total Synthesis; Wiley-VCH: Weinheim, 1996; pp. 582.

2 (*a*) U. H. F. Bunz, *Chem. Rev*., 2000, **100**, 1605; (*b*) D. A. Alonso, C. Najera and M. C. Pacheco, *Tetrahedron Lett*., 2002, **43**, 9365; (*c*) A. L. Rusanov, I. A. Khotina and M. M. Begretov, *Russ. Chem. Rev*., 1997, **66**, 1053.

View Article Online
DOI: 10.1039/C6NJ02771G

3 (*a*) G. Evano, N. Blanchard and M. Toumi, *Chem. Rev*., 2008, **108**, 3054; (*b*) I. P. Beletskaya and A. V. Cheprakov, *Coord. Chem. Rev*., 2004, **248**, 2337; (*c*) F. Monnier and M. Taillefer, *Angew. Chem., Int. Ed*., 2009, **48**, 6954; (*d*) H. Rao and H. Fu, *Synlett*, 2011, 745; (*e*) H. Lin and D. Sun, *Org. Prep. Proced. Int*., 2013, **45**, 341; (*f*) D. S. Surry and S. L. Buchwald, *Chem. Sci*., 2010, **1**, 13; (*g*) E. Sperotto, G. P. M. van Klink, G. van Koten and J. G. de Vries, *Dalton Trans*., 2010, **39**, 10338; (*h*) S. V. Ley and A. W. Thomas, *Angew. Chem., Int. Ed*., 2003, **42**, 5400; (*i*) C. Sambiagio, S. P. Marsden, A. J. Blacker and P. C. McGowan, *Chem. Soc. Rev*., 2014, **43**, 3525; (*j*) Y. N. Kotovshchikov, G. V. Latyshev, N. V. Lukashev and I. P. *Org. Biomol. Chem.,* 2015, **13**, 5542.

4 (*a*) K. Okuro, M. Furuune, M. Enna, M. Miura and M. Nomura, *J. Org. Chem*., 1993, **58**, 4716; (*b*) K. Okuro, M. Furuune, M. Miura and M. Nomura, *Tetrahedron Lett*., 1992, **33**, 5363; (*c*) A. M. Thomas, A. Sujatha and G. Anilkumar, *RSC Adv*., 2014, **4**, 21688.

5 (*a*) Y. Y. Lin, Y. J. Wang, J. H. Cheng and C. F. Lee, *Synlett*., 2012, 930; (*b*) C. H. Lin, Y. J. Wang and C. F. Lee, *Eur. J. Org. Chem*., 2010, 4368; (*c*) X. Qu, T. Li, P. Sun, Y. Zhu, H. Yang and J. Mao, *Org. Biomol. Chem*., 2011, **9**, 6938; (*d*) J. H. Li, B. X. Tang, L. M. Tao, Y. X. Xie, Y. Liang and M. B. Zhang, *J. Org. Chem*., 2006, **71**, 7488.

6 (*a*) E. Zuidema and C. Bolm, *Chem. Eur. J.,* 2010, **16**, 4181; (*b*) Y. Liu, J. Yang and W. Bao, *Eur. J. Org. Chem*., 2009, 5317; (c) J. H. Li, J. L. Li, D. P. Wang, S. F. Pi, Y. X. Xie, M. B. Zhang and X. C. Hu, *J. Org. Chem*., 2007, **72**, 2053; (*d*) M. Wu, J. Mao, J. Guo and S. Ji, *Eur. J. Org. Chem*., 2008, 4050; (*e*) F. Liu and D. Ma, *J. Org. Chem*., 2007, **72**, 4844; (*f*) F. Monnier, F. Turtaut, L. Duroure and M. Taillefer, *Org. Lett*., 2008, **10**, 3203; (*g*) D. Ma and F. Liu, *Chem. Commun*., 2004, 1934; (*h*) S. Priyadarshini, P. J. A. Joseph, P. Srinivas, H. Maheswaran, M. L. Kantam and S. Bhargava, *Tetrahedron Lett*., 2011, **52**, 1615.

View Article Online
DOI: 10.1039/C6NJ02771G

7 (*a*) G. Chen, X. Zhu, J. Cai and Y. Wan, *Synth. Commun*., 2007, **37**, 1355; (*b*) D. Yang, B. Li, H. Yang, H. Fu and L. Hu, *Synlett*, 2011, 702; (*c*) G. Chen, J. Xie, J. Weng, X. Zhu, Z. Zheng, J. Cai and Y. Wan, *Synth. Commun*., 2011, **41**, 3123; (*d*) J. T. Guan, G. A. Yu, L. Chen, T. Q. Weng, J. J. Yuan and S. H. Liu, *Appl. Organometal.Chem*., 2009, **23**, 75.

8 (*a*) C. L. Deng, Y. X. Xie, D. L. Yin and J. H. Li, *Synthesis*., 2006, 3370; (*b*) Y. X. Xie, C. L. Deng, S. F. Pi, J. H. Li and D. L. Yin, *Chin. J. Chem*., 2006, **24**, 1290.

9 (*a*) Y. Zhu, T. Li, X. Qu, P. Sun, H. Yang and J. Mao, *Org. Biomol. Chem*., 2011, **9**, 7309; (*b*) L. X. Shao and M. Shi, *Tetrahedron*, 2007, **63**, 11938.

10 D. J. Vaughan, R. G. Burns and V. M. Burns, *Geochim. Cosmochim. Acta*., 1971, **35**, 365.

11 (*a*) T. Li, H. Li, Z. Wu, H. Hao, J. Liu, T. Huang, H. Sun, J. Zhang, H. Zhang and Z. Guo, *Nanoscale*, 2015, **7**, 4171; (*b*) C. I. Pearce, R. A. D. Pattrick, D. Vaughan, *J. Rev. Mineral. Geochem*., 2006, **61**, 127; (*c*) Y. Zhang, W. Sun, X. Rui, B. Li, H. T. Tan, G. Guo, S. Madhavi, Y. Zong and Q. Yan, *Small,* 2015, **11**, 3694; (*d*) N. Mahmood, C. Zhang, J. Jiang, F. Liu and Y. Hou, *Chem. Eur. J.,* 2013, **19**, 5183; (*e*) Q. Wang, L. Jiao, H. Du, Y. Si, Y. Wang and H. Yuan, *J. Mater. Chem*., 2012, **22**, 21387.

12 A. K. Geim and K. S. Novoselov, *Nature materials*., 2007, **6**, 183.

13 (*a*) T. J. Booth, P. Blake, R. N. Rahul, D. Jiang, E. W. Hill and U. Bangert, *Nano Lett*., 2008, **8**, 2442; (*b*) X. S. Du, Z. Z. Yu, A. Dasari, J. Ma, M. Mo and Y. Z. Meng, *Chem. Mater*., 2008, **20**, 2066; (*c*) D. Li, M. B. Muller, S. Gilje, R. B. Kaner and G. G. Wallace, *Nanotechnology*, 2008, **3**, 101.

14 (*a*) S. J. Hoseini, M. Dehghani and H. Nasrabadi, *Catal. Sci. Technol.*, 2014, **4**, 1078; (*b*) S. J. Hoseini, V. Heidari and H. Nasrabadi, *J. Mol. Catal. A: Chem*., 2015, **396**, 90; (*c*) S. J. Hoseini, H. Ghanavat Khozestan and R. Hashemi Fath, *RSC Adv*., 2015, **5**, 47701; (*d*) N.

View Article Online
DOI: 10.1039/C6NJ02771G

Hussain, A. Borah, G. Darabdhara, P. Gogoi, V. K. Azhagan, M. V. Shelke and M. R. Das, *New J. Chem*., 2015, **39**, 6631.

15 (*a*) W. S. Hummers and R. E. Offeman, *J. Am. Chem. Soc*., 1958, **80**, 1339; (*b*) S. J. Hoseini, M. Bahrami and M. Dehghani, *RSC Adv.,* 2014, **4**, 13796; (*c*) S. J. Hoseini, Z. Barzegar, M. Bahrami, M. Roushani and M. Rashidi, *J. Organomet. Chem*., 2014, **769**, 1.

16 J. Tang, Y. Ge, J. Shen and M. Ye, *Chem. Commun*., 2016, **52**, 1509.

17 C. Feldmann and H. O. Jungk, *Angew. Chem., Int. Ed*., 2001, **40**, 359.

18 (*a*) R. K. Hocking, R. Brimblecombe, L. Y. Chang, A. Singh, M. H. Cheah, C. Glover, W. H. Casey and L. Spiccia, *Nature Chemistry*., 2011, **3**, 461; (*b*) A. S. Arico, P. Bruce, B. Scrosati, J. M. Tarascon and W. Van Schalkwijk, *Nature materials*, 2005, **4**, 366.

19 D. P. Williamson and N. W Grimes, *J. Phys. D: Appl. Phys*., 1974, **7**, 1.

20 (*a*) Y. Dong, L. Wu, G. Wang, H. Zhao, P. Jiang and C. Feng, *Bull. Korean Chem. Soc*., 2013, **34**, 3227; (*b*) T. Saeki, H. Ohktta, N. Kakuta and T. Mizushima, *J. Ceram. Soc. Japan*., 2015, **123**, 955.

21 J. Cheng, H. Yan, Y. Lu, K. Qiu, X. Hou, J. Xu, L. Han, X. Liu, J. K. Kim and Y. Luo, *J. Mater. Chem. A*., 2015, **3**, 9769.

22 (*a*) S. Shekhar and J. F. Hartwig, *J. Am. Chem. Soc*., 2004, **126**, 13016; (*b*) B. Carbonnier, H. B. Romdhane, M. Delamar, M. M. Chehimi, A. B. Gonzalez-Perez, R. Alvarez, O. N. Faza, A. R. de Lera and J. M. Aurrecoechea, *Organometallics.,* 2012, **31**, 2053; (*c*) S. J. Hoseini, A. Zarei and H. Rafatbakhsh Iran, *Appl. Organometal. Chem*., 2015, **29**, 489.

23 A. S. Roy, J. Mondal, B. Banerjee, P. Mondal, A. Bhaumik and S. M. Islam, *Appl. Catal. A: General*., 2014, **469**, 320.

24 M. Esmaeilpour, A. Sardarian and J. Javidi, *Catal. Sci. Technol*., 2016, **6**, 4005.

View Article Online
DOI: 10.1039/C6NJ02771G

25 A. R. Hajipour, S. H. Nazemzadeh and F. Mohammadsaleh, *Tetrahedron Lett.*, 2014, **55**, 654.

26 K. G. Thakur, E. A. Jaseer, A. B. Naidu and G. Sekar, *Tetrahedron Lett.*, 2009, **50**, 2865.

27 J. H. Li, J. L. Li, D. P. Wang, S. F. Pi, Y. X. Xie, M. B. Zhang and X. C. Hu, *J. Org. Chem.*, 2007, **72**, 2053.

28 Y. F. Wang, W. Deng, L. Liu and Q. X. Guo, *Chin. J. Chem.*, 2005, **16**, 1197.

29 C. L. Deng, Y. X. Xie, D. L. Yin and J. H. Li, *Synthesis.*, 2006, **20**, 3370.

DOI: 10.1039/C6NJ02771G

Figure Captions:

Fig. 1 XRD patterns of (a) $CuCo_2S_4$, and (b) $CuCo_2S_4$/RGO nanohybrids.

Fig. 2 XPS curves of $CuCo_2S_4$/RGO nanohybrid (a) Cu 2p and (b) Co 2p.

Fig. 3 (a and b) TEM images of $CuCo_2S_4$/RGO nanohybrid.

Scheme 1 Plausible mechanism of the $CuCo_2S_4$-catalyzed Sonogashira coupling.

Fig. 4 Recycling result of the coupling reaction of bromobenzene with phenylacetylene in the presence of $CuCo_2S_4$ and $CuCo_2S_4$/RGO nanohybrids.

Table Captions:

Table 1 Sonogashira cross-coupling of aryl halides with phenylacetylene catalyzed by the $CuCo_2S_4$ and $CuCo_2S_4$/RGO nanohybrids

Table 2 Solvent and temperature effects on the Sonogashira reaction of chlorobenzene with phenylacetylene catalyzed by the $CuCo_2S_4$/RGO nanohybrid[a]

Table 3 Sonogashira cross-coupling of bromobenzene with phenylacetylene catalyzed by the $Cu(NO_3)_2$, $Cu(NO_3)_2$ + $Co(NO_3)_2$ and $Cu(NO_3)_2$ + $Co(NO_3)_2$ + thiourea[a]

Table 4 Catalytic performance of different Cu-based catalysts in the coupling of bromobenzene and 4-bromotoluene with phenylacetylene

View Article Online
DOI: 10.1039/C6NJ02771G

Table of content:

Synthesis of thiospinel $CuCo_2S_4$ and $CuCo_2S_4$/ reduced-graphene oxide nanohybrids as highly effective catalysts for the Sonogashira reaction†

Roghayeh Hashemi Fath and S. Jafar Hoseini[*]

Department of Chemistry, Faculty of Sciences, Yasouj University, Yasouj 7591874831, Iran

Thiospinel $CuCo_2S_4$ and $CuCo_2S_4$/ reduced-graphene oxide nanohybrids were firstly synthesized through a simple solvothermal approach. Then, these nanohybrids are used as non-phosphine catalysts for the Sonogashira reaction in water.

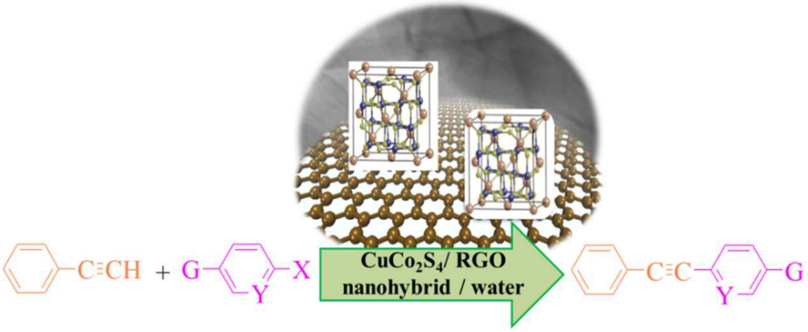

---

[*] Corresponding author: E-mail: jhosseini@yu.ac.ir, sjhoseini54@yahoo.com, Fax: +98 74 33342172; Tel: +98 74 33223048.